Accepted Manuscript

Fractals

Article Title:	Design of neuro-swarming heuristic solver for multi-pantograph singular delay differential equation
Author(s):	Zulqurnain Sabir, Dumitru Baleanu, Muhammad Asif Zahoor Raja, Juan L. G. Guirao
DOI:	10.1142/S0218348X21400223
Received:	11 September 2020
Accepted:	17 December 2020
To be cited as:	Zulqurnain Sabir *et al.*, Design of neuro-swarming heuristic solver for multi-pantograph singular delay differential equation, *Fractals*, doi: 10.1142/S0218348X21400223
Link to final version:	https://doi.org/10.1142/S0218348X21400223

Design of neuro-swarming heuristic solver for multi-pantograph singular delay differential equation

Zulqurnain Sabir[1,a], , Dumitru Baleanu[2, 3, 4, * b] , Muhammad Asif Zahoor Raja[5,6,c], Juan L.G. Guirao[7, d]

[1]*Department of Mathematics and Statistics, Hazara University, Mansehra, Pakista6*
[a] *Email: zulqurnain_maths@hu.edu.pk*

[4]*Department of Mathematics, Cankaya University, Ankara, Turkey*
[5]*Institute of Space Science, Magurele-Bucharest, Romania*
[46]*Department of Medical Research, China Medical University Hospital, China Medical University, Taichung, Taiwan*
**Corresponding author [b]Email: dumitru@cankaya.edu.tr*

[5]*Future Technology Research Center, National Yunlin University of Science and Technology, 123 University Road, Section 3, Douliou, Yunlin 64002, Taiwan, R.O.C.*
[c]*Email: rajamaz@yuntech.edu.tw*
[6]*Department of Electrical and Computer Engineering, COMSATS University Islamabad, Attock Campus, Attock 43600, Pakistan*

[7]*Department of Applied Mathematics and Statistics, Technical University of Cartagena, Hospital de Marina 30203-Cartagena, Spain*

[d]*Email: juan.garcia@upct.es*

Received, 2020
Accepted, 2020
Published

Abstract

The current research work is to design a neural-swarming heuristic procedure for numerical investigations of Singular Multi-Pantograph Delay Differential (SMP-DD) equation by applying the function approximation aptitude of Artificial Neural Networks (ANNs) optimized efficient swarming mechanism based on Particle Swarm Optimization (PSO) integrated with convex optimization with Active Set (AS) algorithm for rapid refinements, named as ANN-PSO-AS, A merit function (MF) on mean squared error sense is designed by using the differential ANN models and boundary condition. The optimization of this MF is executed with the global PSO and local search AS approaches. The planned ANN-PSO-AS approach is instigated for three different SMP-DD model based equations. The assessment with available standard results relieved the effectiveness, robustness and precision that is further authenticated through statistical investigations of Variance Account For, root mean squared error, Semi Interquartile Range and Theil' s inequality coefficient performances.

Keywords: Multi-pantograph systems; Particle swarm optimization, Neural networks; Active-set algorithm; Numerical computing; Statistical measures

1. INTRODUCTION

The singular multi-pantograph delay differential (SMP-DD) equations is considered very important due to its wide-ranging applications in the theory of statistics, physics, electrodynamics, astrophysics, number theory, direction-finding control of ships, engineering, quantum mechanics, finances, chemical sciences, nonlinear dynamical models, chemical kinetics, cell growth, electronic models, infectious viruses and medicine [1-7]. The literature form of the second kind of SMP-DD equation is given as [8]:

$$\begin{aligned} &Y''(\chi)+\sum_{k=1}^{n}\frac{1}{P_k(\chi)}Y'(r_k\chi)+\frac{1}{Q(\chi)}Y(\chi)=G(\chi),\\ &0<\chi,\ r_k<1,\quad k=1,2,3...,n,\\ &Y(0)=A_1,\quad Y'(0)=A_2, \end{aligned} \tag{1}$$

where $P_k(\chi)$ and $Q(\chi)$ are the continuous functions and only a few schemes based on analytical or numerical exist in the literature to solve SMP-DD equation. Some reported studies in this regard for SMP-DD equation can be seen in [9-11]. It is not easy to solve the SMP-DD equation based model (1) due to its harder nature, i.e., multi-pantographs and multi-singular points. All the cited approaches in [9-11] have their specific efficiency, accuracy, performance and limitations. Alongside these mentioned stochastic approaches, the numerical solvers using the heuristic/swarm schemes [12-14] look proficient to integrate the area of multi-pantographs and multi-singular points based nonlinear systems. Some up-to-dated applications of these solvers are nonlinear optics [15], Thomas-Fermi singular model [16], financial market prediction [17], mosquito dispersal model [18], singular three-point model [19], nonlinear system of prey-predator equations [20], singular fourth order model [21], plasma physics problems [22], magnetohydrodynamic studies [23], singular model of Lane-Emden using the Morlet wavelet function [24], fluid dynamics [25], model of heartbeat dynamics [26], corneal shape model [27], multi-singularity based nonlinear models [28], nonlinear models arising in electric circuits [29], nonlinear reactive transport model [30], SIR nonlinear mathematical model for the dynamics of the dengue fever [31], HIV infection model of CD4+ T cells [32], functional differential based singular system [33-34] and nonlinear Riccati equation [35], doubly singular multi-fractional order Lane–Emden system [36], nonlinear unipolar electrohydrodynamic pump flow model [37], future generation disease control mechanism for nonlinear system of COVID-19 epidemic model [38], 3D flow of Eyring-Powell magneto-nanofluidic model [39] and nonlinear dusty plasma system [40]. The aim of this research is to discuss the 2nd order SMP-DD system together with the numerical simulations for superior model understanding using the stochastic approach through Artificial Neural Networks (ANNs) trained with Particle Swarm Optimization (PSO) aided with the Active-Set (AS) algorithm, called as ANN-PSO-AS scheme. Few potential structures of the suggested ANN-PSO-AS algorithm are briefly narrated as follows:

- A novel integrated intelligent approach ANN-PSO-AS is proposed for the numerical treatment of the second order SMP-DD equation based models.
- Overlapping outcomes using the proposed scheme ANN-PSO-AS from reference results for different SMP-DD based examples demonstrated the worth by means of accuracy and convergence indicators.
- Performance of the ANN-PSO-AS solver is endorsed via statistical investigation on multiple executions means of Variance Account For (VAF), root mean square error (RMSE), Semi Interquartile Range (SI-R) and Theil' s inequality coefficient (TIC) performance metrics.
- Beside the accurate outcomes for the second order SMP-DD equation, ease of understanding the concepts, consistency, smooth operation, exhaustive applicability and robustness are other appreciated perks.

The rest of the work is organized as follows: Sect 2 presents the ANN-PSO-AS algorithm; performance indices are provided in Sect 3. The numerical solutions of the second order SMP-DD model is given in Sect 4. Whereas, conclusions and future research plans are given in Sect 5.

2. SOLUTION PROCEDURE:

The framework for solving the second order SMP-DD model is provided in two sections.

- Introducing a mean squared error sense merit/cost function (MF) for solving the differential equation with initial conditions.
- The combination of ANN-PSO-AS algorithm is accessible to optimize the MF for second order SMP-DD model.

2.1 ANN modeling procedures:

The ANNs type of models presented by many researchers to solve the linear/nonlinear structures in various areas [41-42]. The feed-forward ANN based models are used to approximate the continuous mapping solutions and the corresponding derivatives taking the log-sigmoid activation function $S(\chi)=\left(1+\mathrm{e}^{-\chi}\right)^{-1}$ is shown as:

$$\begin{aligned} \hat{Y}(\chi)&=\sum_{i=1}^{k} z_i S(w_i\chi+a_i)=\sum_{i=1}^{k} z_i\left(1+e^{-(w_i\chi+a_i)}\right)^{-1},\\ \hat{Y}'(\chi)&=\sum_{i=1}^{k} z_i S'(w_i\chi+a_i)\\ &=\sum_{i=1}^{k} z_i w_i e^{-(w_i\chi+a_i)}\left(1+e^{-(w_i\chi+a_i)}\right)^{-2},\\ \hat{Y}''(\chi)&=\sum_{i=1}^{k} z_i S''(w_i\chi+a_i)\\ &=\sum_{i=1}^{k} z_i w_i^2\begin{pmatrix} 2e^{-2(w_i\chi+a_i)}\left(1+e^{-(w_i\chi+a_i)}\right)^{-3}-\\ e^{-(w_i\chi+a_i)}\left(1+e^{-(w_i\chi+a_i)}\right)^{-2}\end{pmatrix}, \end{aligned} \tag{2}$$

where the weights are $\boldsymbol{z}=[z_1,z_2,z_3,...,z_m]$, $\boldsymbol{w}=[w_1,w_2,w_3,...,w_m]$ and $\boldsymbol{a}=[a_1,a_2,a_3,...a_m]$. For solving the second order SMP-DD model presented in equation (1), an error-based function is introduced as follows:

$$e_{FIT}=e_{FIT-1}+e_{FIT-2}, \tag{3}$$

where e_{FIT-1} and e_{FIT-2} are an unsupervised error functions related to second order SMP-DD model and initial conditions, given as:

$$e_{FIT-1} = \frac{1}{N}\sum_{i=1}^{N}\left(\hat{Y}_i'' + \sum_{k=1}^{n}\frac{1}{P_{k,i}}\hat{Y}_{k,i}' + \frac{1}{Q_i}\hat{Y}_i - G_i\right)^2, \quad r_k < 1,\ k = 1,2,...,n,\ i = 1,2,...,N \tag{4}$$

where $Nh = 1,\ P_{k,i} = P_i(\chi_k),\ Q_i = Q(\chi_i), \hat{Y}_i = \hat{Y}(\chi_i),$. $\hat{Y}_{k,i} = \hat{Y}(r_k\chi_i),\ \chi_i = kh$. Similarly, e_{FIT-2} is the error function associated to the initial conditions, written as:

$$e_{FIT-2} = \frac{1}{2}\left((\hat{Y}_0)^2 + (\hat{Y}_N)^2\right). \tag{5}$$

2.2 Network Optimization: PSO-AS approach

The combined framework of PSO and AS approach ratifies the optimization of the parameters for solving the second order SMP-DD model given in equation (1).

There are many global search schemes, among them PSO is a well-known global search algorithm used as an optimization solver. PSO works as an alteration of genetic algorithm process, which is introduced by Eberhart and Kennedy in the previous century [43-44]. It is metaheuristic in nature due to its optimization capabilities in large search spaces. The execution process of the PSO as compared to GA is relatively efficient to implement due to the less memory requirement. In the optimization of PSO approach, initial swarm spreads in the larger domain. To improve the PSO, the procedure gives iteratively optimal results $\boldsymbol{P}_{LB}^{\phi-1}$ and $\boldsymbol{P}_{GB}^{\phi-1}$, which designate the position and velocity of the swarm, written as:

$$\boldsymbol{X}_i^{\phi} = \boldsymbol{X}_i^{\phi-1} + \boldsymbol{V}_i^{\phi-1}, \tag{6}$$

$$\boldsymbol{V}_i^{\phi} = \Psi \boldsymbol{V}_i^{\phi-1} + \phi_1(\boldsymbol{P}_{LB}^{\phi-1} - \boldsymbol{X}_i^{\phi-1})\boldsymbol{r}_1 + \phi_2(\boldsymbol{P}_{GB}^{\phi-1} - \boldsymbol{X}_i^{\phi-1})\boldsymbol{r}_2, \tag{7}$$

where Ψ is the inertia weight vector, X_i is the position and V_i represents velocity. Whereas, ϕ_1 and ϕ_2 are the constant for acceleration factors.

PSO has widespread applications in parameter estimation of plane waves [45], nonlinear electric circuits [46], nonlinear optimization problems [47], reactive power dispatch problems [48], active-noise control systems [49], optimization in atomic power plants [50] and design of novel epidemic models [51].

The convergence performance of the PSO scheme is boosted by the hybridization of a local search technique. In this regard, "active-set" (AS) algorithm is used for quick modification of the results. Active-set is a valuable scheme that confines the system model for better understanding along with optimization of the proposed system. Recently, AS method is applied for convex unconstrained and constrained optimization problems reported in [52-55].

In this work, the PSO-AS method is functional to present the solution of the second order SMP-DD model provided in equation (1). The detail of the pseudocode using the ANN-PSO-AS method is tabulated in Table 1.

3. PERFORMANCE METRICS:

The section presents the mathematical form of the statistical operators based on VAF, RMSE and TIC for solving three variants of second order SMP-DD system. The mathematical forms are introduced as:

$$\begin{cases} VAF = \left(1 - \dfrac{\operatorname{var}\left(Y_i(\chi) - \hat{Y}_i(\chi)\right)}{\operatorname{var}\left(Y_i(\chi)\right)}\right) * 100, \\ EVAF = \left|VAF - 100\right|, \end{cases} \tag{8}$$

$$\text{RMSE} = \sqrt{\frac{1}{n}\sum_{i=1}^{n}\left(Y_i - \hat{Y}_i\right)^2} \tag{9}$$

$$\text{TIC} = \frac{\sqrt{\frac{1}{n}\sum_{i=1}^{n}\left(Y_i - \hat{Y}_i\right)^2}}{\left(\sqrt{\frac{1}{n}\sum_{i=1}^{n}Y_i^2} + \sqrt{\frac{1}{n}\sum_{i=1}^{n}\hat{Y}_i^2}\right)}, \tag{10}$$

Table 1: Optimization process using the designed ANN-PSO-AS approach

```
Start of PSO
...Step 1: Initialization: Randomly generate the primary swarms. Transform the parameters of the
      'PSO' and 'optimoptions'.
...Step 2: Fitness formulation: Using equation (3), scrutinize the ''fitness values'' of each
      particle.
.   Step 3: Ranking: Rank individually the particle for minimum values of the "Merit function".
.   Step 4: Stopping Standards: Dismiss if
      •  "Fitness level" accomplished.
      •  Selected "flights/cycles" executed.
      When "stopping" standard meets, move to Step 5
.   Step 5: Renewal: By using equations (6) and (7), call the "position" and "velocity"
.   Step 6: Improvement: Repeat the step (2)→(6), until the whole 'flights' are achieved.
...Step 7: Storage: Save the best "Merit function values", represented as "best global particle"
PSO process Ends

Start the PSO-AS approach
      Inputs: Global best values
      Output: W_PSO-AS signifies the best PSO-AS approach values
      Initialize: Used "Global best values" as a start point
      Termination: Stop if {Fitness=e_FIT =10^-18},{Generation=700},
```

{TolCon = TolX = TolFun = 10^{-21}} and {MaxFunEvals = 275000} gets the above standards.
While {Stop}
Calculation of Fitness: Use e_{FIT} for the "fitness values" given in equation (3)
Adjustments: Invoke the 'fmincon' routine for the AS approach to finetune the values of the "weight vector".
Move to "fitness step" using the "weight vector's" updated form.
Store: Store the $\mathbf{W}_{\mathbf{PSO\text{-}AS}}$, iterations, e_{FIT}, function count and time for the present trial.
PSO-AS approach Ends

4. RESULTS AND DISCUSSIONS: The detailed discussion of the results to solve three different examples based on second order SMP-DD model is provided in this section.

Example I: Consider the second order SMP-DD equation involving exponential functions is written as:

$$\begin{aligned} &Y''(\chi)+\frac{1}{\chi}Y'\left(\frac{\chi}{2}\right)+\frac{1}{\chi^2}Y'\left(\frac{\chi}{4}\right)+\frac{1}{1-\chi}Y(\chi)=H(\chi),\\ &0<\chi\le 1,\\ &Y(0)=1,\ Y'(0)=1, \end{aligned} \tag{11}$$

where

$$H(\chi)=-\frac{\left(e^{\frac{\chi}{4}}(\chi-1)\right)}{4}-\frac{\left(\chi e^{\frac{\chi}{2}}(\chi-1)\right)}{2}-e^{\chi}(\chi-2)\chi^2.$$

The exact solution of the second order SMP-DD equation (11) is e^{χ} and the MF function becomes as:

$$e_{FIT}=\frac{1}{N}\sum_{m=1}^{N}\begin{pmatrix}\chi_m^2(1-\chi_m)\hat{Y}''(\chi_m)+\\ \chi_m(1-\chi_m)\hat{Y}'\left(\frac{1}{2}\chi_m\right)+\\ (1-\chi_m)\hat{Y}'\left(\frac{1}{4}\chi_m\right)+\\ \chi_m^2F_m-\chi_m^2(1-\chi_m)H_m\end{pmatrix}^2 +\frac{1}{2}\left(\left(\hat{Y}_0-1\right)^2+\left(\hat{Y}_0'-1\right)^2\right) \tag{12}$$

Example II: Let a 2nd order SMP-DD system with trigonometric expressions as:

$$\begin{aligned} &Y''(\chi)+\frac{1}{\chi}Y'\left(\frac{\chi}{2}\right)+\frac{1}{\chi^2}Y'\left(\frac{\chi}{4}\right)+\frac{1}{1-\chi}Y(\chi)=R(\chi),\\ &0<\chi\le 1,\\ &Y(0)=1,\ Y'(0)=0, \end{aligned} \tag{13}$$

where $R(\chi)=\dfrac{\chi}{1-\chi}\cos\chi-\dfrac{1}{\chi}\sin\left(\dfrac{\chi}{2}\right)-\dfrac{1}{\chi^2}\sin\left(\dfrac{\chi}{4}\right).$

The exact solution of the second order SMP-DD equation (13) is $Cos(\chi)$ and the MF function becomes as:

$$e_{FIT}=\frac{1}{N}\sum_{m=1}^{N}\begin{pmatrix}\chi_m^2(1-\chi_m)\hat{Y}''(\chi_m)+\\ \chi_m(1-\chi_m)\hat{Y}'\left(\frac{1}{2}\chi_m\right)+\\ (1-\chi_m)\hat{Y}'\left(\frac{1}{4}\chi_m\right)+\\ \chi_m^2F_m-\chi_m^2(1-\chi_m)R_m\end{pmatrix}^2 +\frac{1}{2}\left(\left(\hat{Y}_0-1\right)^2+\left(\hat{Y}_0'\right)^2\right). \tag{14}$$

Example III: Let a 2nd order SMP-DD system with hyperbolic trigonometric expressions as:

$$\begin{aligned} &Y''(\chi)+\frac{1}{\chi}Y'\left(\frac{\chi}{2}\right)+\frac{1}{\chi^2}Y'\left(\frac{\chi}{4}\right)+\frac{1}{1-\chi}Y(\chi)=G(\chi),\\ &0<\chi\le 1,\\ &Y(0)=0,\ Y'(0)=1, \end{aligned} \tag{15}$$

where

$$G(\chi)=\frac{2-\chi}{1-\chi}Sinh(\chi)+\frac{1}{\chi}Cosh\left(\frac{\chi}{2}\right)+\frac{1}{\chi^2}Cosh\left(\frac{\chi}{4}\right).$$

The exact solution of the second order SMP-DD equation (15) is $\sinh(\chi)$ and the MF function becomes as:

$$e_{FIT}=\frac{1}{N}\sum_{m=1}^{N}\begin{pmatrix}\chi_m^2(1-\chi_m)\hat{Y}''(\chi_m)+\\ \chi_m(1-\chi_m)\hat{Y}'\left(\frac{1}{2}\chi_m\right)+\\ (1-\chi_m)\hat{Y}'\left(\frac{1}{4}\chi_m\right)+\\ \chi_m^2F_m-\chi_m^2(1-\chi_m)G_m\end{pmatrix}^2 +\frac{1}{2}\left(\left(\hat{Y}_0\right)^2+\left(\hat{Y}_0'-1\right)^2\right). \tag{16}$$

The designed ANN-PSO-AS approach is applied for sixty runs to get the system parameters using the ANN-PSO-AS to solve the second order SMP-DD model-based Examples I, II and III. The set of trained decision variables that are used to demonstrate the estimated numerical solution of the model (1). The mathematical formulation of the projected solutions is written as:

$$\hat{Y}_1(\chi)=\frac{5.9788}{1+e^{-(1.143\chi+7.658)}}+\frac{1.6700}{1+e^{-(-4.767\chi-7.766)}}+\frac{9.0929}{1+e^{-(1.064\chi-2.228)}}+\ldots+\frac{3.2410}{1+e^{-(3.636\chi-8.395)}}, \tag{17}$$

$$\hat{Y}_2(\chi)=\frac{0.2002}{1+e^{-(4.177\chi+0.622)}}+\frac{11.7221}{1+e^{-(4.137\chi-12.892)}}+\frac{-6.536}{1+e^{-(11.822\chi+11.817)}}+\ldots-\frac{0.9502}{1+e^{-(-11.802\chi-9.837)}}, \tag{18}$$

$$\hat{Y}_3(\chi)=\frac{-3.8295}{1+e^{-(-2.323\chi-6.028)}}-\frac{6.4774}{1+e^{-(-2.045\chi+6.163)}}+\frac{4.3507}{1+e^{-(0.7494\chi+1.013)}}+\ldots-\frac{1.7718}{1+e^{-(2.227\chi-8.666)}}. \tag{19}$$

Optimization is performed to solve the second order SMP-DD model-based problems I-III for the interval [0, 1] with 0.05 step size applying the PSO-AS hybridization for 60 independent executions. A best weights set and the exact, mean and proposed results comparison for the second order SMP-DD model-based examples I-III are provided in figure 1. It is observed that for all the examples, all the said solutions overlapped with each other. This coinciding of the outcomes indicates the perfection of the ANN-PSO-AS approach. The values of the absolute error (AE) and performance investigations through ANN-PSO-AS approach for second order SMP-DD model-based examples I-III are plotted in figure 2. The values of the AE are plotted in subfigures 2(a-c), while the performance measures are drawn 2(d-f).

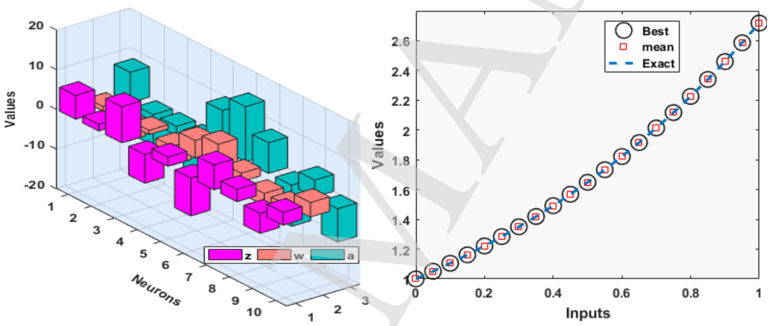

(a) Example 1: Best weights

(d) Example 1: Result comparison

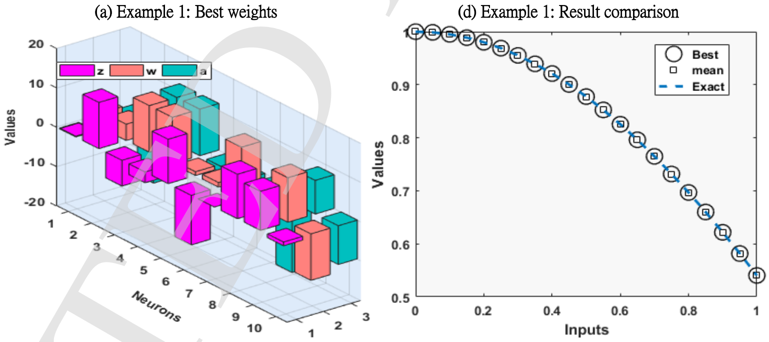

(b) Example 2: Best weights

(e) Example 2: Result comparison

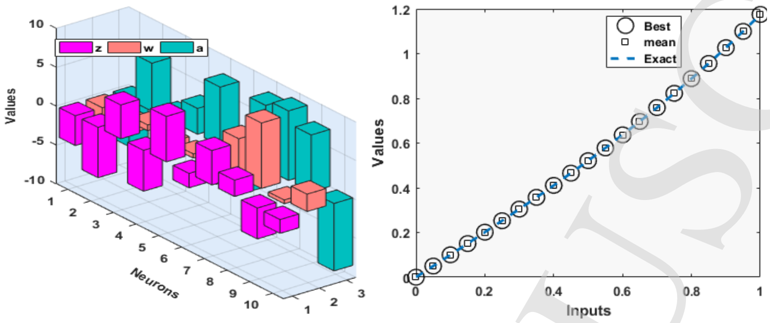

(c) Example 3: Best weights (f) Example 3: Result comparison

Figure 1: A best weights set along with the exact, mean and proposed solutions of the second order SMP-DD model-based examples I-III

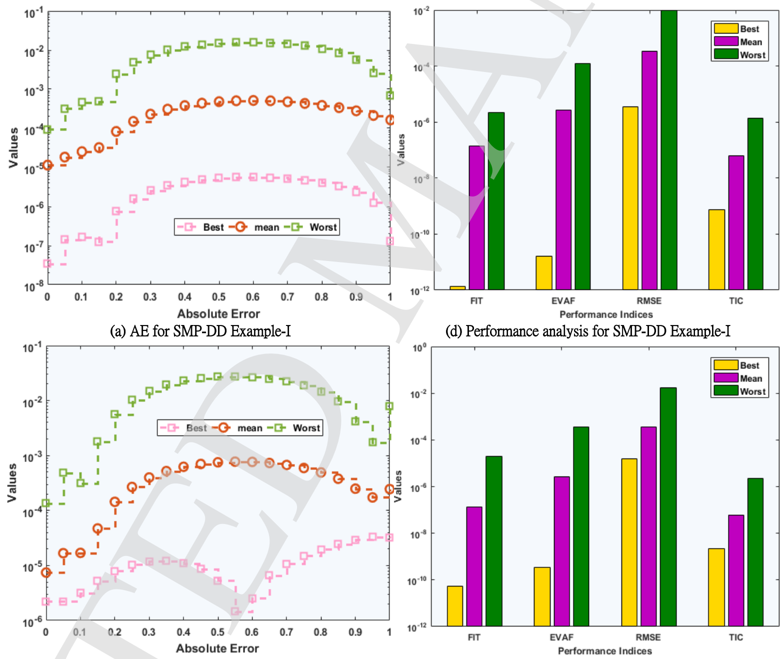

(a) AE for SMP-DD Example-I

(d) Performance analysis for SMP-DD Example-I

(b) AE for SMP-DD Example-II

(e) Performance analysis for SMP-DD Example-II

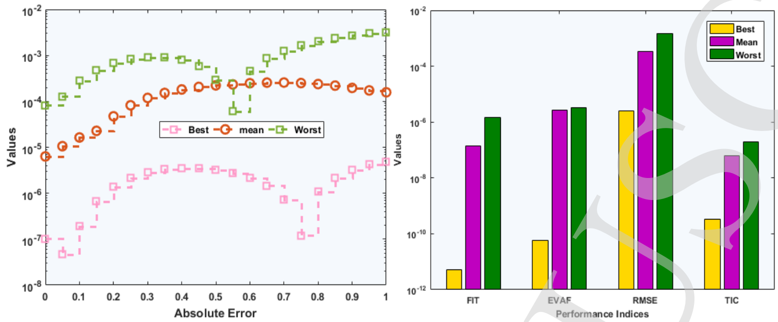

(c) AE for SMP-DD Example-III (f) Performance analysis for SMP-DD Example-III

Figure 2: The AE along with other performance metrics of ANN-PSO-AS approach for second order SMP-DD model-based examples I-III

It is seen that the best values for example I, II and III are found near to 10^{-6} to 10^{-7}, 10^{-5} to 10^{-6} and 10^{-6} to 10^{-7}, while the mean and worst for all the examples are found around 10^{-4} to 10^{-5} and 10^{-2} to 10^{-4}, respectively. The best fitness and EVAF for all the examples observed near to 10^{-9} to 10^{-12}, while for all examples, the best RMSE and TIC lie 10^{-4} to 10^{-6} and 10^{-8} to 10^{-10}, respectively. The mean Fitness and TIC values for all the examples are about 10^{-6} to 10^{-8}, while the mean for EVAF and RMSE lie around 10^{-4} to 10^{-6} and 10^{-2} to 10^{-4}, respectively. Moreover, even the worst indices for all the gages are also found to be satisfactory.

The statistical investigation for ANN-PSO-AS approach via Fitness, EVAF, RMSE and TIC operators together with the boxplots/histogram values for SMP-DD model-based examples I to III are provided in figures 3 to 6. These statistical studies are accomplished for 60 independent executions using 10 numbers of neurons. It is seen, the Fitness, EVAF, RMSE and TIC values lie around 10^{-06} to 10^{-10}, 10^{-07} to 10^{-09}, 10^{-03} to 10^{-05} and 10^{-07} to 10^{-09}, respectively.

For accuracy analysis of the ANN-PSO-AS designed approach, statistical values are accomplished for 60 executions using minimum (Min), Mean, semi interquartile range (SI-R) and median (MED) to solve the second order SMP-DD model-based examples I to III. SI-R is the $0.5*(Q_3-Q_1)$, where Q_1 and Q_3 are the respective first and third quartiles. The Min, Mean, SI-R and MED statistic measures are given in Table 2 to solve the SMP-DD equations. It is indicated that the Min values lie 10^{-06} to 10^{-08}, 10^{-06} to 10^{-09} and 10^{-06} to 10^{-08} ranges for example I-III. The mean and MED and SI-R values are found in the 10^{-04} to 10^{-06} region for all examples. These values stipulate very good measures for the SMP-DD model.

Table 2: Statistics results for the second order SMP-DD model based Examples I-III

χ	Example I				Example II				Example III			
	Min	Mean	MED	SI-R	Min	Mean	MED	SI-R	Min	Mean	MED	SI-R
0	3×10^{-08}	1×10^{-05}	1×10^{-06}	1×10^{-06}	7×10^{-08}	7×10^{-06}	2×10^{-06}	2×10^{-06}	4×10^{-08}	6×10^{-06}	1×10^{-06}	2×10^{-06}
0.05	5×10^{-08}	1×10^{-05}	4×10^{-06}	4×10^{-06}	2×10^{-07}	1×10^{-05}	4×10^{-06}	3×10^{-06}	4×10^{-08}	1×10^{-05}	4×10^{-06}	2×10^{-06}
0.1	1×10^{-07}	2×10^{-05}	6×10^{-06}	5×10^{-06}	1×10^{-07}	1×10^{-05}	7×10^{-06}	5×10^{-06}	1×10^{-07}	1×10^{-05}	5×10^{-06}	4×10^{-06}
0.15	5×10^{-08}	3×10^{-05}	6×10^{-06}	7×10^{-06}	2×10^{-07}	4×10^{-05}	1×10^{-05}	7×10^{-06}	6×10^{-08}	2×10^{-05}	7×10^{-06}	6×10^{-06}
0.2	2×10^{-07}	8×10^{-05}	2×10^{-05}	1×10^{-05}	3×10^{-07}	1×10^{-04}	3×10^{-05}	2×10^{-05}	3×10^{-08}	4×10^{-05}	1×10^{-05}	2×10^{-05}
0.25	1×10^{-06}	1×10^{-04}	3×10^{-05}	3×10^{-05}	1×10^{-06}	2×10^{-04}	5×10^{-05}	4×10^{-05}	2×10^{-06}	8×10^{-05}	4×10^{-05}	3×10^{-05}
0.3	1×10^{-06}	2×10^{-04}	6×10^{-05}	5×10^{-05}	1×10^{-07}	4×10^{-04}	8×10^{-05}	6×10^{-05}	2×10^{-06}	1×10^{-04}	6×10^{-05}	4×10^{-05}
0.35	3×10^{-07}	3×10^{-04}	8×10^{-05}	7×10^{-05}	5×10^{-06}	5×10^{-04}	1×10^{-04}	8×10^{-05}	6×10^{-07}	1×10^{-04}	9×10^{-05}	6×10^{-05}
0.4	1×10^{-07}	3×10^{-04}	9×10^{-05}	8×10^{-05}	6×10^{-06}	6×10^{-04}	1×10^{-04}	1×10^{-04}	3×10^{-06}	1×10^{-04}	1×10^{-04}	7×10^{-05}
0.45	5×10^{-08}	4×10^{-04}	1×10^{-04}	1×10^{-04}	3x10-09	7×10^{-04}	1×10^{-04}	1×10^{-04}	2×10^{-06}	2×10^{-04}	1×10^{-04}	8×10^{-05}
0.5	4×10^{-06}	4×10^{-04}	1×10^{-04}	1×10^{-04}	5×10^{-06}	7×10^{-04}	1×10^{-04}	1×10^{-04}	1×10^{-06}	2×10^{-04}	1×10^{-04}	8×10^{-05}
0.55	3×10^{-06}	5×10^{-04}	1×10^{-04}	1×10^{-04}	1×10^{-06}	7×10^{-04}	2×10^{-04}	1×10^{-04}	4×10^{-07}	2×10^{-04}	1×10^{-04}	8×10^{-05}
0.6	2×10^{-06}	5×10^{-04}	1×10^{-04}	1×10^{-04}	1×10^{-06}	7×10^{-04}	2×10^{-04}	1×10^{-04}	7×10^{-08}	2×10^{-04}	1×10^{-04}	1×10^{-04}
0.65	1×10^{-06}	5×10^{-04}	1×10^{-04}	1×10^{-04}	6×10^{-06}	7×10^{-04}	2×10^{-04}	1×10^{-04}	1×10^{-06}	2×10^{-04}	1×10^{-04}	1×10^{-04}
0.7	1×10^{-07}	4×10^{-04}	1×10^{-04}	1×10^{-04}	6×10^{-06}	6×10^{-04}	2×10^{-04}	1×10^{-04}	7×10^{-07}	2×10^{-04}	1×10^{-04}	9×10^{-05}
0.75	1×10^{-06}	4×10^{-04}	1×10^{-04}	1×10^{-04}	5×10^{-06}	5×10^{-04}	1×10^{-04}	1×10^{-04}	1×10^{-07}	2×10^{-04}	1×10^{-04}	8×10^{-05}
0.8	3×10^{-06}	3×10^{-04}	1×10^{-04}	1×10^{-04}	7×10^{-06}	4×10^{-04}	1×10^{-04}	9×10^{-05}	1×10^{-06}	2×10^{-04}	1×10^{-04}	8×10^{-05}

0.85	2×10^{-06}	3×10^{-04}	9×10^{-05}	9×10^{-05}	1×10^{-06}	3×10^{-04}	1×10^{-04}	7×10^{-05}	3×10^{-08}	2×10^{-04}	1×10^{-04}	8×10^{-05}
0.9	2×10^{-06}	2×10^{-04}	6×10^{-05}	7×10^{-05}	2×10^{-06}	2×10^{-04}	1×10^{-04}	9×10^{-05}	3×10^{-06}	2×10^{-04}	1×10^{-04}	9×10^{-05}
0.95	8×10^{-07}	2×10^{-04}	5×10^{-05}	6×10^{-05}	1x10-10	1×10^{-04}	8×10^{-05}	9×10^{-05}	1×10^{-08}	1×10^{-04}	9×10^{-05}	7×10^{-05}
1	1×10^{-07}	1×10^{-04}	3×10^{-05}	6×10^{-05}	2×10^{-06}	2×10^{-04}	6×10^{-05}	7×10^{-05}	5×10^{-07}	1×10^{-04}	8×10^{-05}	6×10^{-05}

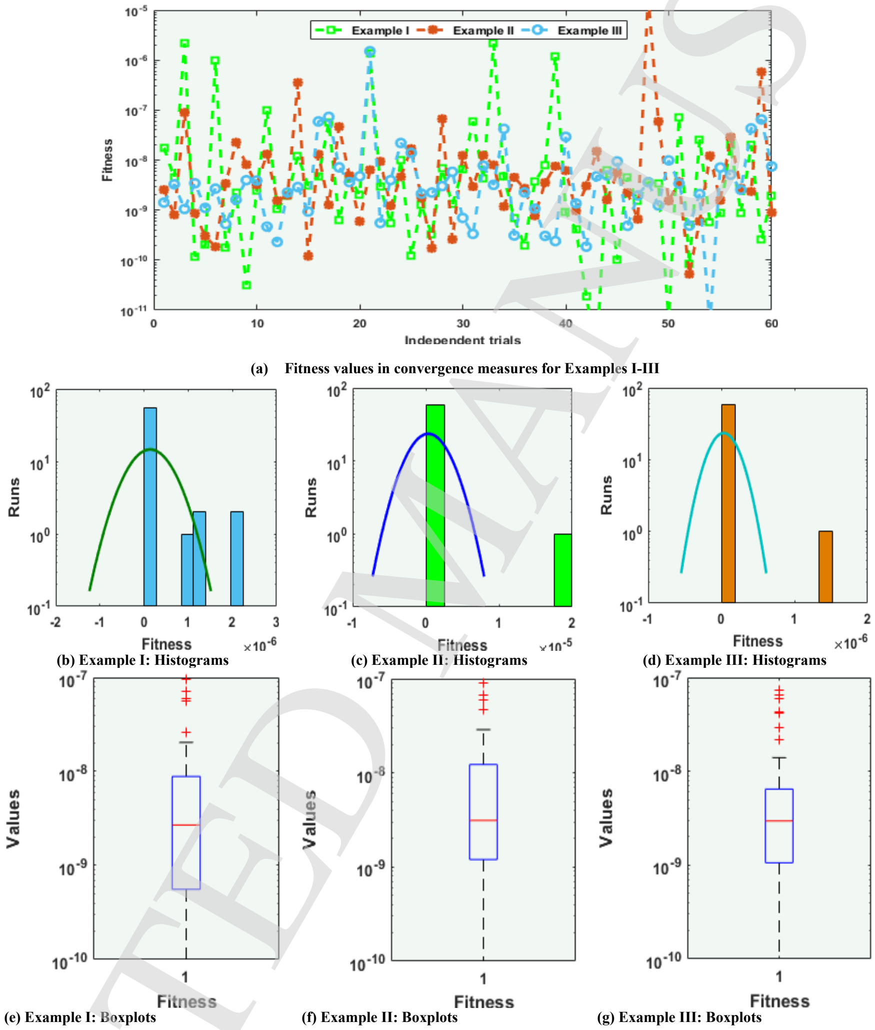

(a) Fitness values in convergence measures for Examples I-III

(b) Example I: Histograms (c) Example II: Histograms (d) Example III: Histograms

(e) Example I: Boxplots (f) Example II: Boxplots (g) Example III: Boxplots

Figure 3: Statistical assessments on ANN-PSO-AS approach via fitness together with the boxplots/histograms for SMP-DD model-based examples I to III.

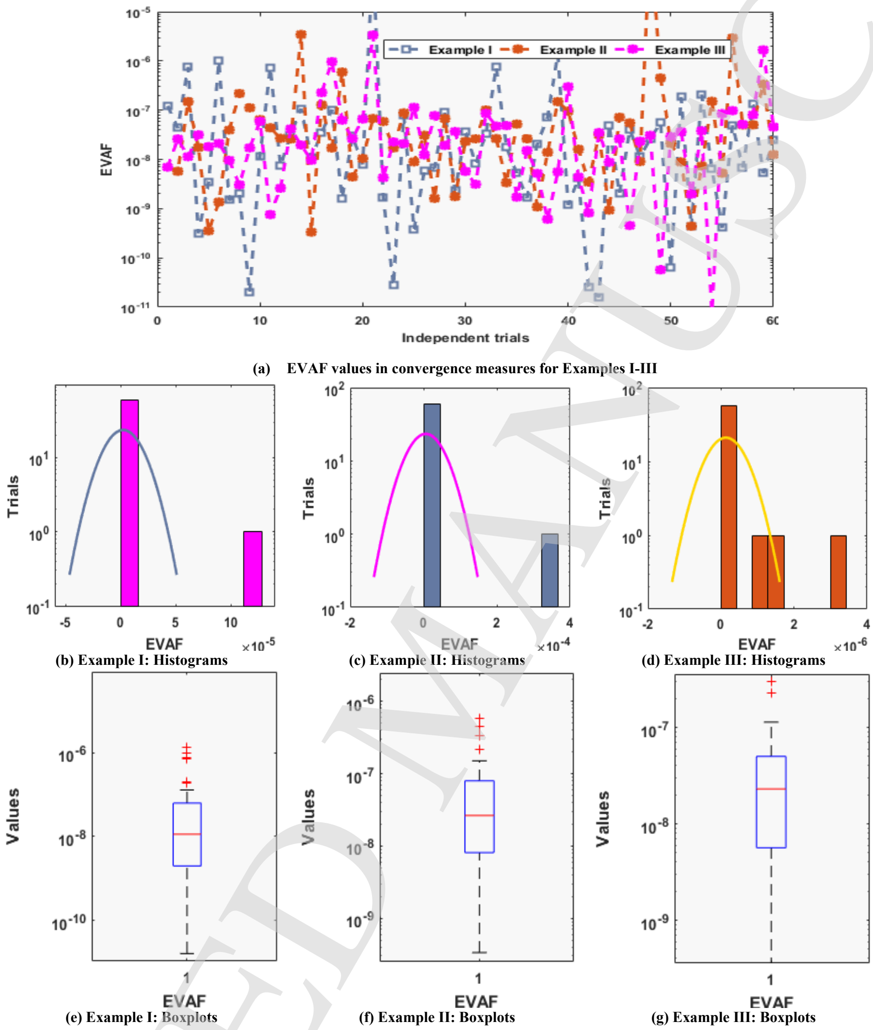

(a) EVAF values in convergence measures for Examples I-III

(b) Example I: Histograms

(c) Example II: Histograms

(d) Example III: Histograms

(e) Example I: Boxplots

(f) Example II: Boxplots

(g) Example III: Boxplots

Figure 4: Statistical assessments on ANN-PSO-AS approach via EVAF together with the boxplots/histograms for SMP-DD model-based examples I to III.

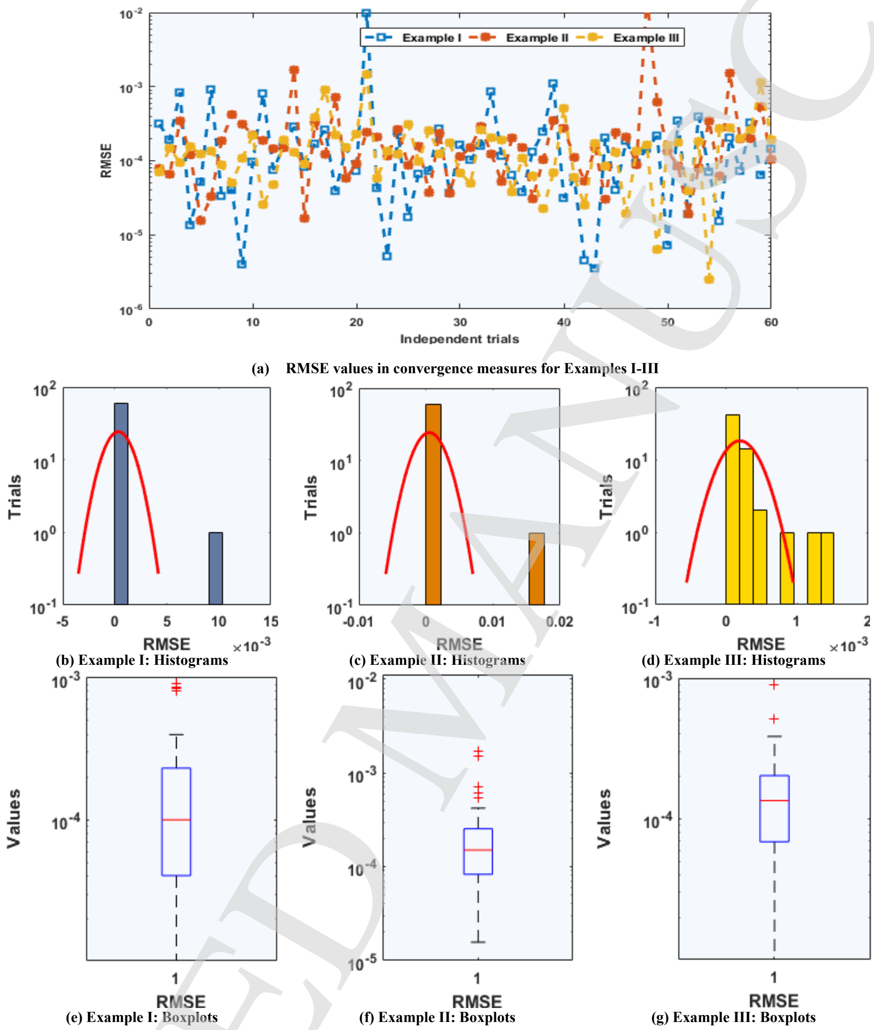

Figure 5: Statistical assessments on ANN-PSO-AS approach via RMSE together with the boxplots/histograms for SMP-DD model-based examples I to III.

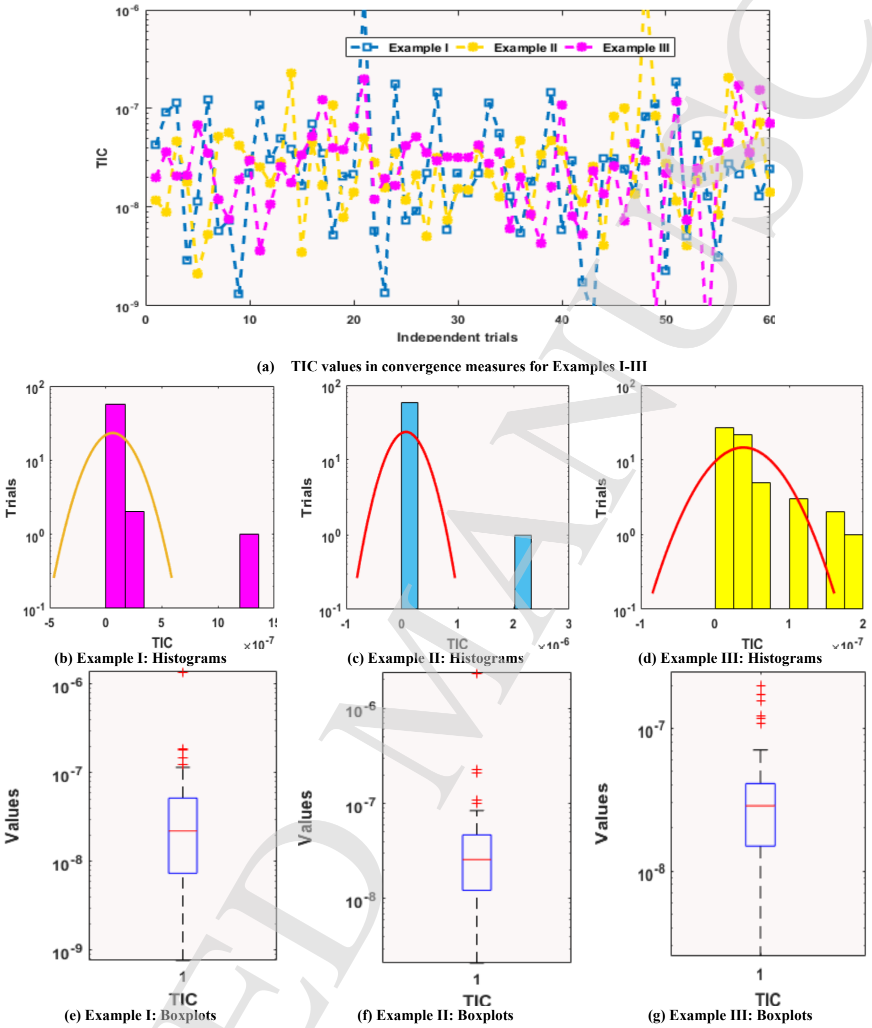

Figure 6: Statistical assessments on ANN-PSO-AS approach via TIC together with the boxplots/histograms for SMP-DD model-based examples I to III.

4. CONCLUSION: The design of the numerical computing solver ANN-PSO-AS is presented to solve 2nd order singular multi-pantograph delay differential system and the outcomes are precise, stable and consistent using the ANNs competency of regression. A merit function of the networks is designed based on the error function and accordingly optimization with local and global capabilities of the active-set approach and particle swarm optimization, respectively. The ANN-PSO-AS approach is accomplished to solve 3 different examples of the second order singular multi-pantograph delay differential model. The precise performance of ANN-PSO-AS approach is verified through AE within reasonable accuracy, i.e., around 6 to 8 decimals of precision from the true/exact outcomes for all variants of the singular multi-pantograph delay differential equations. The statistical investigations on Min, SI-R, Mean and MED indices further certified the robustness, stability and precision of ANN-PSO-AS approach for solving the second order singular multi-pantograph delay differential system.

In the future, the ANN-PSO-AS algorithm based accurate stochastic numerical procedure can be implemented on for higher order functional differential model [56-57], computer virus models [58-59], mathematical model for information security [60-61], bioinformatics [62-63] and dynamical analysis of computational fluid mechanics problems [64-66].

Conflict of interest: All the authors of the manuscript declared that there are no potential conflicts of interest.

REFERENCES

[1] Leonid Bogachev, Gregory Derfel, Stanislav Molchanov, and John Ochendon. On bounded solutions of the balanced generalized pantograph equation. In Pao-Liu Chow, George Yin, and Boris Mordukhovich, editors, Topics in Stochastic Analysis and Nonparametric Estimation, volume 145 of The IMA Volumes in Mathematics and its Applications, pages 29 – 49. Springer New York, 2008.

[2] Soleymani Karimi Vanani, Sedighi Hafshejani and Khan. On the numerical solution of generalized pantograph equation. World Applied Sciences Journal, 13(12):2531 – 2535, 2011.

[3] M. Z. Liu, D.S. Li, Properties of analytic solution and numerical solution of multi-pantograph equation, Appl.Math.Comput,155(2004),853-871.

[4] M.Sezer, A method for approximate solution of the second order linear differential equation in terms of Taylor polynomials,Internat. J. Math,447-468.

[5] Petio Kelevedjiev, Existence of positive solutions to a singular second order boundary value problem. Nonlinear Analysis, 50(2002), 1107-1118.

[6] Y.S. Liu, H.M. Yu, Existence and uniquess of positive solution for singular boundary value problem. Computers and Mathematics with Applications, 50 (2005),133-143.

[7] M.Sezer, Salih yalcinbas, Niyazi Sahin, Approximate solution of multi-pantograph equation with variable coefficients. Computational and Mathematics, 7 (2007),1-11.

[8] Du, P. and Geng, F., 2008. A new method of solving singular multi-pantograph delay differential equation in reproducing kernel space. Appl. Math. Sci, 27(2), pp.1299-1305.

[9] Bahgat, M.S., 2020. Approximate analytical solution of the linear and nonlinear multi-pantograph delay differential equations. *Physica Scripta*, *95*(5), p.055219.

[10] Yousefi, S.A., Noei-Khorshidi, M. and Lotfi, A., 2018. Convergence analysis of least squares-Epsilon-Ritz algorithm for solving a general class of pantograph equations. *Kragujevac Journal of Mathematics*, *42*(3), pp.431-439.

[11] Yang, Y. and Tohidi, E., 2019. Numerical solution of multi-Pantograph delay boundary value problems via an efficient approach with the convergence analysis. *Computational and Applied Mathematics*, *38*(3), p.127.

[12] Raja, M.A.Z., Khan, J.A., Zameer, A., Khan, N.A. and Manzar, M.A., 2019. Numerical treatment of nonlinear singular Flierl–Petviashivili systems using neural networks models. *Neural Computing and Applications*, **31**, pp.2371 – 2394.

[13] Raja, M.A.Z., Abbas, S., Syam, M.I. and Wazwaz, A.M., 2018. Design of neuro-evolutionary model for solving nonlinear singularly perturbed boundary value problems. *Applied Soft Computing*, *62*, pp.373-394.

[14] Zúñiga-Aguilar, C.J., Coronel-Escamilla, A., Gómez-Aguilar, J.F., Alvarado-Martínez, V.M. and Romero-Ugalde, H.M., 2018. New numerical approximation for solving fractional delay differential equations of variable order using artificial neural networks. *The European Physical Journal Plus*, *133*(2), p.75.

[15] Ahmad, I., et al., 2018. Neuro-evolutionary computing paradigm for Painlevé equation-II in nonlinear optics. *The European Physical Journal Plus*, *133*(5), p.184.

[16] Sabir, Z., et al., 2018. Neuro-heuristics for nonlinear singular Thomas-Fermi systems. Applied Soft Computing, 65, pp.152-169.

[17] Bukhari, A.H., et al., 2020. Fractional Neuro-Sequential ARFIMA-LSTM for Financial Market Forecasting. *IEEE Access*.

[18] Umar, M., et al., 2020. A stochastic computational intelligent solver for numerical treatment of mosquito dispersal model in a heterogeneous environment. The European Physical Journal Plus, 135(7), pp.1-23.

[19] Sabir, Z., Baleanu, D., Shoaib, M. *et al.* Design of stochastic numerical solver for the solution of singular three-point second-order boundary value problems. *Neural Comput & Applic* (2020). https://doi.org/10.1007/s00521-020-05143-8.

[20] Umar, M., et al., 2019. Intelligent computing for numerical treatment of nonlinear prey–predator models. Applied Soft Computing, 80, pp.506-524.

[21] Sabir, Z., et al., 2020. Heuristic computing technique for numerical solutions of nonlinear fourth order Emden–Fowler equation. *Mathematics and Computers in Simulation*, *178*, pp.534-548.

[22] Raja, M.A.Z., Shah, F.H., Tariq, M. and Ahmad, I., 2018. Design of artificial neural network models optimized with sequential quadratic programming to study the dynamics of nonlinear Troesch's problem arising in plasma physics. Neural Computing and Applications, 29(6), pp.83-109.

[23] Mehmood, A., et al., 2018. Design of neuro-computing paradigms for nonlinear nanofluidic systems of MHD Jeffery–Hamel flow. *Journal of the Taiwan Institute of Chemical Engineers*, *91*, pp.57-85.

[24] Sabir, Z., et al., 2020. Novel design of Morlet wavelet neural network for solving second order Lane–Emden equation. *Mathematics and Computers in Simulation*, *172*, pp.1-14..

[25] Mehmood, A., et al., 2018. Intelligent computing to analyze the dynamics of magnetohydrodynamic flow over stretchable rotating disk model. *Applied Soft Computing*, *67*, pp.8-28.

[26] Raja, M. A. Z., Shah, F. H., Alaidarous, E. S. and Syam, M. I., 2017. Design of bio-inspired heuristic technique integrated with interior-point algorithm to analyze the dynamics of heartbeat model. Applied Soft Computing, 52, pp. 605-629.

[27] Ahmad, I., *et al.* Integrated neuro-evolution-based computing solver for dynamics of nonlinear corneal shape model numerically. *Neural Comput & Applic* (2020). https://doi.org/10.1007/s00521-020-05355-y.

[28] Raja, M.A.Z., Mehmood, J., Sabir, Z., Nasab, A.K. and Manzar, M.A., 2019. Numerical solution of doubly singular nonlinear systems using neural networks-based integrated intelligent computing. Neural Computing and Applications, 31(3), pp.793-812.

[29] Mehmood, A., et al., 2019. Integrated

computational intelligent paradigm for nonlinear electric circuit models using neural networks, genetic algorithms and sequential quadratic programming. *Neural Computing and Applications*, DOI: https://doi.org/10.1007/s00521-019-04573-3

[30] Ahmad, I., et al., 2019. Novel applications of intelligent computing paradigms for the analysis of nonlinear reactive transport model of the fluid in soft tissues and microvessels. *Neural Computing and Applications*, *31*(12), pp.9041-9059.

[31] Umar, M., et al., 2020. A stochastic numerical computing heuristic of SIR nonlinear model based on dengue fever. *Results in Physics*, p.103585.

[32] Umar, M., et al., 2020. Stochastic numerical technique for solving HIV infection model of CD4+ T cells. The European Physical Journal Plus, 135(6), p.403.

[33] Sabir, Z., et al., 2020. Neuro-swarm intelligent computing to solve the second-order singular functional differential model. The European Physical Journal Plus, 135(6), p.474.

[34] Sabir, Z., Wahab, H.A., Umar, M. and Erdoğan, F., 2019. Stochastic numerical approach for solving second order nonlinear singular functional differential equation. Applied Mathematics and Computation, 363, p.124605.

[35] Raja, M.A.Z., Manzar, M.A. and Samar, R., 2015. An efficient computational intelligence approach for solving fractional order Riccati equations using ANN and SQP. *Applied Mathematical Modelling*, *39*(10-11), pp.3075-3093.

[36] Sabir, Z., et al., 2020. FMNEICS: fractional Meyer neuro-evolution-based intelligent computing solver for doubly singular multi-fractional order Lane – Emden system. *Computational and Applied Mathematics*, *39*(4), pp.1-18.

[37] Jadoon, I., et al., 2020. Integrated meta-heuristics finite difference method for the dynamics of nonlinear unipolar electrohydrodynamic pump flow model. *Applied Soft Computing*, *97*, p.106791.

[38] Cheema, T.N., et al., 2020. Intelligent computing with Levenberg – Marquardt artificial neural networks for nonlinear system of COVID-19 epidemic model for future generation disease control. *The European Physical Journal Plus*, *135*(11), pp.1-35.

[39] Shah, Z., et al., 2020. Design of neural network based intelligent computing for numerical treatment of unsteady 3D flow of Eyring-Powell magneto-nanofluidic model. *Journal of Materials Research and Technology*, *9*(6), pp.14372-14387.

[40] Bukhari, A.H., et al., 2020. Design of a hybrid NAR-RBFs neural network for nonlinear dusty plasma system. *Alexandria Engineering Journal*, *59*(5), pp.3325-3345.

[41] Taheri, M.H., Abbasi, M. and Jamei, M.K., 2019. Application of an artificial neural network to predict the entrance length of three-dimensional magnetohydrodynamics channel flow. *The European Physical Journal Plus*, *134*(9), p.471.

[42] Nasirzadehroshenin, F., Sadeghzadeh, M., Khadang, A., Maddah, H., Ahmadi, M.H., Sakhaeinia, H. and Chen, L., 2020. Modeling of heat transfer performance of carbon nanotube nanofluid in a tube with fixed wall temperature by using ANN – GA. *The European Physical Journal Plus*, *135*(2), pp.1-20.

[43] Brezočnik, L., Fister, I. and Podgorelec, V., 2018. Swarm intelligence algorithms for feature selection: a review. *Applied Sciences*, *8*(9), p.1521.

[44] Zedadra, O., Guerrieri, A., Jouandeau, N., Spezzano, G., Seridi, H. and Fortino, G., 2018. Swarm intelligence-based algorithms within IoT-based systems: A review. *Journal of Parallel and Distributed Computing*, *122*, pp.173-187.

[45] Akbar, S., et al., 2019. Novel application of FO-DPSO for 2-D parameter estimation of electromagnetic plane waves. *Neural Computing and Applications*, *31*(8), pp.3681-3690.

[46] Mehmood, A., et al., 2019. Design of nature-inspired heuristic paradigm for systems in nonlinear electrical circuits. Neural Computing and Applications, pp.1-17.

[47] Duary, A., Rahman, M.S., Shaikh, A.A., Niaki, S.T.A. and Bhunia, A.K., 2020. A new hybrid algorithm to solve bound-constrained nonlinear optimization problems. Neural Computing and Applications, pp.1-26.

[48] Muhammad, Y., Khan, R., Ullah, F. *et al.* Design of fractional swarming strategy for solution of optimal reactive power dispatch. *Neural Comput & Applic* **32,** 10501 – 10518 (2020). https://doi.org/10.1007/s00521-019-04589-9.

[49] Raja, M.A.Z., Aslam, M.S., Chaudhary, N.I., Nawaz, M. and Shah, S.M., 2019. Design of hybrid nature-inspired heuristics with application to active noise control systems. *Neural Computing and Applications*, *31*(7), pp.2563-2591.

[50] Zameer, A., et al., 2020. Fractional-order particle swarm based multi-objective PWR core loading pattern optimization. *Annals of Nuclear Energy*, *135*, p.106982.

[51] Fan, D., Jiang, G.P., Song, Y.R., Li, Y.W. and Chen, G., 2019. Novel epidemic models on PSO-based networks. *Journal of theoretical biology*, *477*, pp.36-43.

[52] Koehler, S., Danielson, C. and Borrelli, F., 2017. A primal-dual active-set method for distributed model predictive control. Optimal Control Applications and Methods, 38(3), pp. 399-419.

[53] Wang, X. and Pardalos, P. M., 2017. A modified active set algorithm for transportation discrete network design bi-level problem. Journal of Global Optimization, 67(1-2), pp. 325-342.

[54] Shen, C., Zhang, L. H. and Yang, W. H., 2016. A Filter Active-Set Algorithm for Ball/Sphere Constrained Optimization Problem. SIAM Journal on Optimization, 26(3), pp. 1429-1464.

[55] Azizi, M., Amirfakhrian, M. and Araghi, M.A.F., 2020. A fuzzy system based active set algorithm for the numerical solution of the optimal control problem governed by partial differential equation. *European Journal of Control*, *54*, pp.99-110.

[56] Khan, I., et al., 2020. Design of Neural Network with Levenberg-Marquardt and Bayesian Regularization Backpropagation for Solving Pantograph Delay Differential Equations. *IEEE Access*, *8*, pp.137918-137933.

[57] Raja, M.A.Z., Ahmad, I., Khan, I., Syam, M.I. and Wazwaz, A.M., 2017. Neuro-heuristic computational intelligence for solving nonlinear pantograph systems. *Frontiers of Information Technology & Electronic Engineering*, *18*(4), pp.464-484.

[58] Masood, Z., et al., 2018. Design of Epidemic Computer Virus Model with Effect of Quarantine in the Presence of Immunity. *Fundamenta Informaticae*, *161*(3), pp.249-273.

[59] Raza, A., Arif, M.S., Rafiq, M., Bibi, M., Naveed,

M., Iqbal, M.U., Butt, Z., Naseem, H.A. and Abbasi, J.N., 2019. Numerical treatment for stochastic computer virus model. *Computer Modeling in Engineering & Sciences*, *120*(2), pp.445-465.

[60] Masood, Z., et al., 2019. Design of a mathematical model for the Stuxnet virus in a network of critical control infrastructure. *Computers & Security*, *87*, p.101565.

[61] Masood, Z., et al., 2020. Design of fractional order epidemic model for future generation tiny hardware implants. *Future Generation Computer Systems*, *106*, pp.43-54.

[62] Umar, M., et al., 2020. A Stochastic Intelligent Computing with Neuro-Evolution Heuristics for Nonlinear SITR System of Novel COVID-19 Dynamics. *Symmetry*, *12*(10), p.1628.

[63] Raja, M.A.Z., Umar, M., Sabir, Z., Khan, J.A. and Baleanu, D., 2018. A new stochastic computing paradigm for the dynamics of nonlinear singular heat conduction model of the human head. *The European Physical Journal Plus*, *133*(9), p.364.

[64] Umar, M. et al., 2019. Three-dimensional flow of Casson nanofluid over a stretched sheet with chemical reactions, velocity slip, thermal radiation and Brownian motion. Thermal Science, (00), pp.339-339.

[65] Sabir, Z., et al., 2019. A Computational Analysis of Two-Phase Casson Nanofluid Passing a Stretching Sheet Using Chemical Reactions and Gyrotactic Microorganisms. Mathematical Problems in Engineering, 2019.

[66] Imran, A., et al., 2019. Analysis of MHD and heat transfer effects with variable viscosity through ductus efferentes. *AIP Advances*, *9*(8), p.085320.